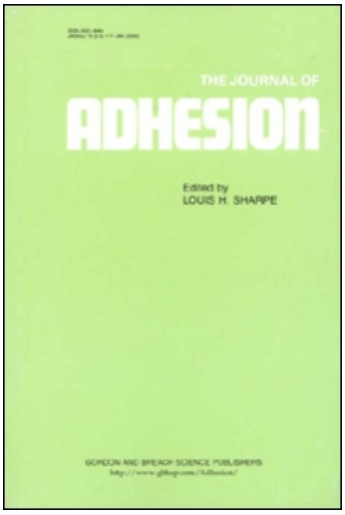

The Journal of Adhesion
Publication details, including instructions for authors and subscription information:
http://www.informaworld.com/smpp/title~content=t713453635

Effect of Adhesive Ductility on Cyclic Debond Mechanism in Composite-to-Composite Bonded Joints

S. Mall[a]; K. T. Yun[b]
[a] Department of Aeronautics and Astronautics, Air Force lnsitute of Technology, OH, U.S.A. [b] Department of Aerospace Engineering and Engineering Mechanics, University of Texas, Austin, TX, U.S.A.

To cite this Article Mall, S. and Yun, K. T.(1987) 'Effect of Adhesive Ductility on Cyclic Debond Mechanism in Composite-to-Composite Bonded Joints', The Journal of Adhesion, 23: 4, 215 — 231
To link to this Article: DOI: 10.1080/00218468708075408
URL: http://dx.doi.org/10.1080/00218468708075408

J. Adhesion, 1987, Vol. 23, pp. 215–231
Photocopying permitted by license only

Printed in the United Kingdom

Effect of Adhesive Ductility on Cyclic Debond Mechanism in Composite-to-Composite Bonded Joints †

S. MALL

Department of Aeronautics and Astronautics, Air Force Insitute of Technology, Wright-Patterson Air Force Base, OH 45433-6583, U.S.A.

K. T. YUN

Department of Aerospace Engineering and Engineering Mechanics, University of Texas, Austin TX 78712, U.S.A.

(Received June 6, 1986)

An investigation of an adhesively bonded composite joint with a brittle adhesive was conducted to characterize both the static and fatigue debond growth mechanism under mode *I* and mixed mode *I–II* loadings. The bonded system consisted of graphite/epoxy adherends bonded with FM-400 adhesive. Two specimen types were tested: (1) a double-cantilever-beam specimen for mode *I* loading and (2) a cracked-lap-shear specimen for mixed mode *I–II* loading. In all specimens tested, failure occurred in the form of debond growth either in a cohesive or adhesive manner. The total strain-energy-release rate is not the criterion for cohesive debond growth under static and fatigue loading in the birttle adhesive as observed in previous studies with the ductile adhesives. Furthermore, the relative fatigue resistance and threshold value of cyclic debond growth in terms of its static fracture strength is higher in the brittle adhesive than its counterpart in the ductile adhesive.

KEY WORDS Adhesive bonding; composite materials; debond propagation; strain-energy-release rates; fracture mechanics; fatigue.

† Presented at the Tenth Annual Meeting of The Adhesion Society, Inc., Williamsburg, Virginia, U.S.A., February 22–27, 1987.

INTRODUCTION

Adhesive bonds have several major advantages relative to mechanical fastenings, including potential savings in weight and in manufacturing costs. It has a special attraction in joining of fiber reinforced composite structural components since it eliminates the cutting of fibers as well as holes and stress concentration associated with them. Thus, substantial weight savings can be realized which is a major reason for selecting composite materials for structural components. If the advantages of adhesviely bonded joints, as compared to mechanically fastened joints, are to be fully exploited, a thorough understanding is required of failure mechanism in terms of service environmental regimes, including cyclic mechanical load, both load and application time, temperature and humidity. In this paper, attention will be focused on fatigue load environment.

One of first tasks in an effective study of the fatigue of any structure is to define the possible modes of damage propagation. In joints with mechanical fasteners, the growth of a crack from a fastener is the principal mode of damage. When an adhesively bonded joint is subjected to fatigue loading, one of the possible damage modes that can occur, is called cyclic debond—progressive separation of the adherends by failure of the adhesive bond under cyclic load. Roderick, *et al.*[1] and Mostovoy and Ripling[2] were the first to study cycling debonding in bonded joints. Roderick, *et al.* studied the cyclic debond phenomenon in composite-to-metal joints under in-plane, mixed-mode constant amplitude loading, while Mostovoy and Ripling investigated the cyclic debonding under opening mode alternating loads. These early studies showed that the correlations between cyclic debond growth rate and corresponding strain-energy-release rate resulted in the same sigmoidal shapes that had been previously observed in studies of fatigue crack propagation in metals.

Later on, Marceau, *et al.*[3] found that the cyclic debond growth rate is influenced by temperature and moisture, and Jablonski[4] investigated the crack closure effects on fatigue crack growth in a bondline under mode I condition. Brussat, *et al.*[5] developed the crack-lap-shear specimen to study the effect of mixed-mode loading on adhesive joints. Romanko, *et al.*[6] extended these fracture

mechanics concepts to investigate the fatigue failure of adhesive joints under various environmental condition involving temperature, moisture, etc. However, the correlations between debond growth rates and fracture mechanics parameters from this study[6] were completed by Lin and Liechti.[7] To assess the repeatability of debond growth rates in adhesively bonded joints subjected to constant-amplitude cyclic loading, a study was recently undertaken by Everett and Johnson.[8] Everett has also investigated the role of peel stresses in cyclic debonding.[9]

Besides, the above mentioned studies, the first author and his colleagues have conducted several studies involving the fatigue failure behavior of adhesive bonds between composite adherends.[10–12] In these studies, cyclic debonding was investigated under opening mode *I* and in-plane mixed-mode *I–II* loading. For this purpose, graphite/epoxy double-cantilever–beam (DCB) and cracked-lap-shear (CLS) specimens were tested under constant-amplitude cyclic loading in an ambient laboratory environment. These studies showed that the relations G_I *versus* da/dN from the DCB specimens and G_T *versus* da/dN from the CLS specimens agreed with each other, where G_I is the total (and also opening mode I) strain-energy-release rate for DCB specimens, and G_T is the total strain-energy-release rate for CLS specimens. The relation G_I *versus* da/dN from the CLS specimen under mixed-mode loading did not, however, agree with the relation G_I *versus* da/dN from the DCB specimen under the opening mode I loading. The results of these studies, thus, showed that the cyclic debond failure in the adhesively bonded composite joints is governed by the total strain-energy-release rate.

In these studies[10–12] two adhesives were used: EC 3445 (3M) and FM-300 (Bloomindale Div., American Cyanamid). Both these adhesives are rubber toughened epoxy structural adhesives, and are ductile adhesives. These studies were extended to investigate the effect of adhesive properties (*i.e.*, brittle *versus* ductile adhesives) on the cyclic debond mechanism. This was the objective of the present study. For this purpose, graphite/epoxy double-cantilever-beam and cracked-lap-shear specimens were tested using FM-400 (American Cyanamid) which is a relatively more brittle adhesive. This investigation focused on the correlation of the measured cyclic

debond growth rate with the corresponding strain-energy-release rate. The present study as well as previous studies, thus, provided the data to evaluate the effect of adhesive ductility on the cyclic debond mechanism.

SPECIMEN FABRICATION AND CONFIGURATION

Two specimen types were fabricated: DCB and CLS specimens, as shown in Figures 1 and 2. The DCB and CLS specimens were used to characterize debond growth under opening mode I loading and mixed-mode loading, respectively. The DCB and CLS specimen

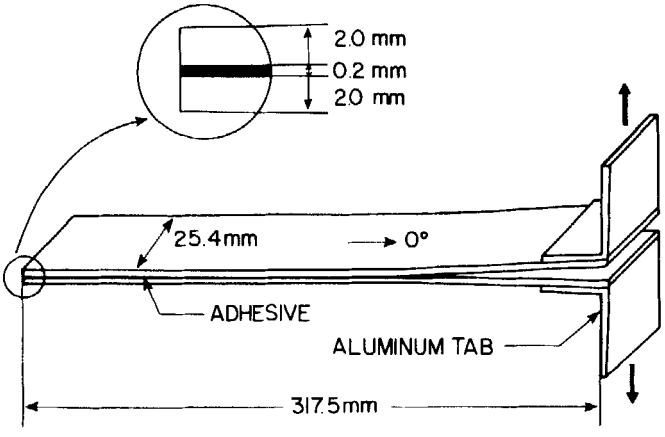

FIGURE 1 Double-cantilever-beam specimen.

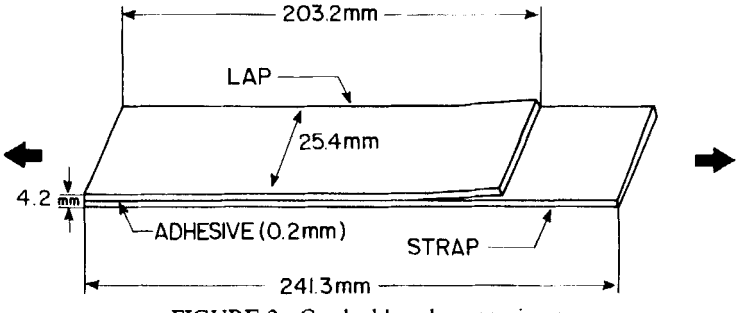

FIGURE 2 Cracked-lap-shear specimen.

consisted of two bonded graphite/epoxy (T300/5208; NARMCO Corp.) adherends, each having 15 unidirectional plies with an initial debond length of 38 mm. This debond was introduced by a Teflon film equal to the adhesive bondline. Two 0.5 mm thick aluminum ends tabs were bonded to the DCB specimen. The peeling load was applied through these tabs. The bonding was done as per manufacturers' recommended procedure. The nominal adhesive thickness was 0.2 mm.

EXPERIMENTS

The experimental program included the static and fatigue tests for both DCB and CLS specimens. The purpose of this program was to measure the critical strain-energy-release rate under the static loading, and to measure the debond growth rate under the cyclic loading. These are already described in details in Ref. 11, where a similar study was carried on with EC 3445 and FM-300 adhesives as mentioned earlier. A brief description of the experimental program is given in the following for the sake of completeness.

DCB specimen

Both static and fatigue tests of the DCB specimen were conducted in the displacement test mode. Prior to testing, either for static or fatigue loading, these specimens were fatigued to create a debond of at least 6 mm beyond the end of Teflon film. The static tests involved the application of displacement at a slow crosshead speed (1.0 cm/min). The critical load corresponding to onset of debond growth was measured carefully. The debond occurred in the stable manner which resulted in the deviation from linearity in the measured load *versus* cross-head displacement relation. This was also verified by a clip-gage near the debond front. After each static test, the specimen was fatigued until the debond grew at least 6 mm further, thus forming a sharp crack for the next static test. A series of static tests were performed on each specimen, which provided the averaged value of G_{IC} for each specimen as per the procedure described in Ref. 11.

The fatigue tests of DCB specimens were performed at a cyclic

frequency of 2 Hz and a stress ratio of 0.1 under constant amplitude cyclic displacement. During fatigue tests debond lengths, fatigue cycles, applied loads, and displacements were monitored continuously. The measured relation between the debond length and fatigue cycle provided the debond growth rate, da/dN. The strain-energy-release rate G_I associated with the cyclic debonding was computed as per the procedure discribed in Ref. 11.

CLS specimen

Static tests of CLS specimen were conducted in the displacement test mode. Prior to testing, the specimen was fatigued to create an initial sharp debond. The critical load corresponding to unstable debond growth was measured from the recorded load-displacement curve. The debond growth resulted in the deviation in the load-displacement cruve. The displacement was measured with two displacement transducers attached on the opposite side of the specimen. Only one measurement could be obtained from each specimen, since the debond grew into the composite strap adherend.

Fatigue tests of CLS specimens were conducted under constant amplitude cyclic load at 2 Hz frequency and stress ratio, $R = 0.1$. Debond lengths and fatigue cycles were monitored continuously throughout the test. The measured relation between the debond length and fatigue cycles provided the debond growth rate, da/dN. Tests were conducted at two or more constant amplitude stress levels to get several values of debond growth rates from each specimen. The tested CLS specimens were analyzed with the finite element program to compute strain-energy-release rates for both static and fatigue loading, as explained in the following section.

FINITE ELEMENT ANALYSIS

A geometric nonlinear finite element program, GAMNAS,[13] was used to analyze the tested CLS specimens in order to account for the nonlinearity associated with the large rotations in the unsymmetric CLS specimen. A typical finite-element model (FEM) of a cracked-lap-shear specimen is shown in Figure 3. This FEM mesh

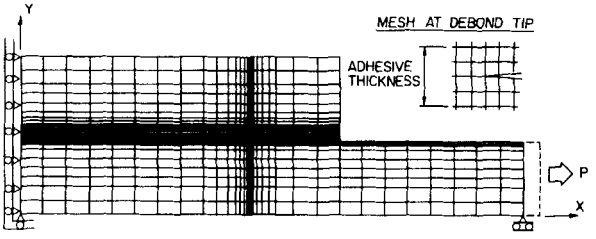

FIGURE 3 Finite element mesh (Y Coordinates are magnified 20 ×).

consisted of about 1200 isoparametric 4-node elements and had about 2400 degrees of freedom. A multipoint constraint was applied to the loaded end of the model to prevent rotation (*i.e.*, all of the axial displacements along the ends are equal to simulate actual grip loading of the specimen). Plane-strain condition was assumed in the analysis. The material properties of composite adherend and adhesive are listed in Tables I and II. The strain-energy-release rate was computed using a virtual crack-closure technique.[14]

TABLE I
Graphite/epoxy[a] adherend material properties[b]

Modulus,[c] GPa			Poisson's ratio[c]	
E_{11}	E_{22}	G_{12}	ν_{12}	ν_{23}
131.0	13.0	6.4	0.34	0.35

[a] T300/5208, fiber volume fraction = 0.63
[b] $E_{33} = E_{22}$, $\nu_{13} = \nu_{12}$, $G_{13} = G_{12}$
[c] The subscripts 1, 2 and 3 correspond to the longitudinal, transverse and thickness directions, respectively, of an unidirectional ply.

The previous study[10] indicated that at least 12 elements were required through the adhesive thickness to reach convergence on G_I and G_{II} calculations. However, the calculation of G_T was not affected by the number of elements through the adhesive thickness.

TABLE II
Adhesive material properties

Adhesive	Modulus, GPa		Poisson's ratio
	E	G	ν
FM-400	4.83	1.72	0.4

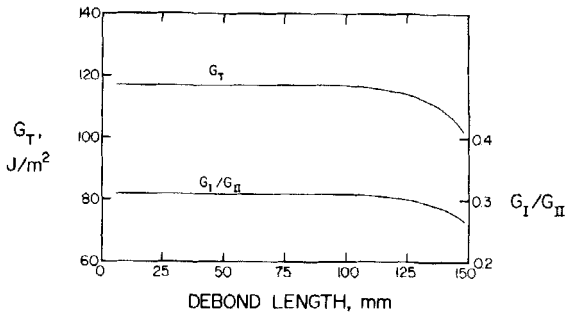

FIGURE 4 Variation of strain-energy-release rates with debond length for the applied stress of 175 MPa.

Further, it was found that G_T was not affected by the location of debond through the adhesive thickness, *i.e.*, whether it was cohesive or adhesive failure. On the other hand, G_I/G_{II} varied slightly with the location of the debond through the adhesive thickness. The focus of the present study was not to investigate the interaction of mixed mode loading on cycling debonding like the previous studies[10–12] but to study the effect of adhesive ductility on cyclic debond behavior. For this purpose, four elements through the adhesive thickness were considered sufficient to calculate the strain-energy-release rates for the tested CLS specimens. The debond was modeled at the middle of the adhesive thickness. Figure 4 shows the variation of the computed strain-energy-release rates G_T and G_I/G_{II} with the debond length.

ADHESIVE DETAILS

This section will present the background information regarding the adhesive FM-400 used in the present study as well as of FM-300 and EC 3445 adhesives used in the previous studies,[10–12] in order to discuss the results of the present study as well as previous studies in this context.

FM-400 is a modified epoxy adhesive film with an aluminum filler and a light weight nylon carrier. On the other hand, FM-300 and EC 3445 are rubber-modified, epoxy structural adhesives. FM-300 is a mat-reinforced film adhesive, while EC 3445 is a one-part paste.

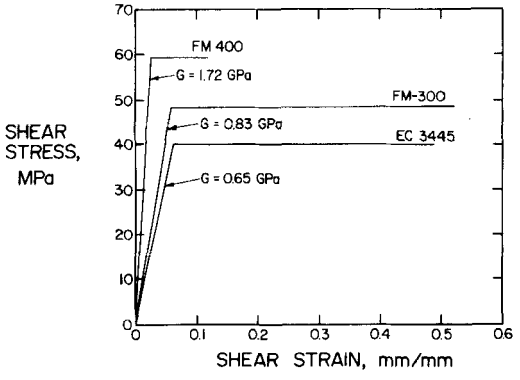

FIGURE 5 Comparison of shear stress–strain response of three adhesives.

All three adhesives are currently being used in the aerospace industry. Due to differences in chemistry and reinforcement (rigid *versus* flexible), FM-400 has a higher strength and modulus than compared to FM-300 and EC 3445. Further, FM-400 is of a comparatively more brittle type than FM-300 and EC 3445 which are more ductile. Hence, FM-400 adhesive will be referred as a brittle adhesive, while FM-300 and EC 3445 will be referred as ductile adhesives. These characteristics are depicted in terms of bondline shear stress and shear strain relations in Figure 5. These stress-strain relations were measured with a thick adherend specimen and were obtained from the manufacturers of these adhesives. These are the average representation of adhesives bondline behavior at room temperature, and not the exact behavior. Therefore, they are represented as an elastic-perfectly plastic material instead of having the usual nonlinear behavior, as commonly observed.

RESULTS AND DISCUSSIONS

Debond locations

All DCB and CLS specimens tested in the present study with FM-400 failed by debond propagation during both static and fatigue tests. The debond grew either in a cohesive manner (*i.e.*, within adhesive) or adhesive manner (*i.e.*, at, or near, the adherend-

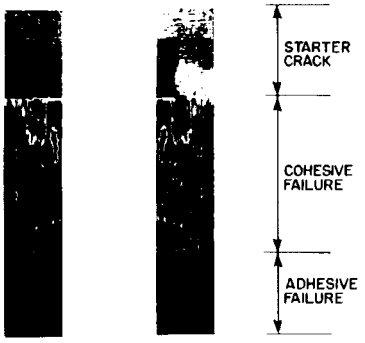

FIGURE 6 Debonded surfaces of double-cantilever-beam specimen.

adhesive interface). There was no consistent pattern for this behavior. In both specimens, it was observed that once debond growth occurred in the adhesive manner, it continued in that manner. However, if it grew in the cohesive manner, it continued in that manner or sometimes it changed to the adhesive type of failure. Typical debond surfaces with these failure details are shown in Figures 6 and 7. The sudden transition from cohesive to adhesive failure in the adhesive bondline with scrim cloth can be probably attributed to weak bonds between the mat carrier and the adhesive (either poorly bonded or not chemically bonded) which provided the crack growth path toward the interface. And, once debond growth occurred in adhesive manner, it continued in that manner since it is the weakest link in the tested bonded system.

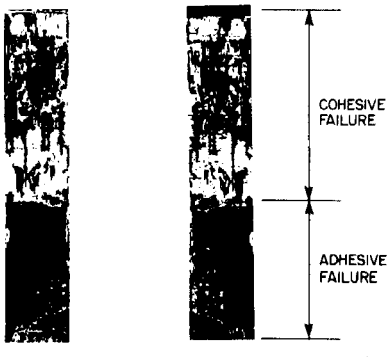

FIGURE 7 Debonded surfaces of cracked-lap-shear specimen.

Thus, the presence of scrim or mat carrier may weaken a bonded joint. This effect has been investigated in a thick adherend model joint, in a qualitative way, in a previous study.[15]

The above mentioned debond growth characteristic was also observed in the DCB specimen with FM-300 where the debond propagated in an irregular manner during both static and fatigue tests involving cohesive, adhesive, or mixed cohesive-adhesive debonding. However, CLS specimens with FM-300 debonded in a cohesive manner only during static and fatigue tests. On the other hand, with adhesive EC 3445 (without any carrier cloth), the debond propagated in a cohesive manner for both specimens (DCB and CLS) and loadings (static and fatigue).[10–11] Further, in CLS specimens with FM-400 in the present study, as well as with FM-300 and EC 3445 adhesives in the previous study,[10] the debond was always closer to the strap than the lap adherend. A possible explanation for this debond characteristic has been investigated with the finite element analysis in the previous study.[10]

Static debonding behavior

Table III presents the critical strain-energy-release rates G_{IC} and $G_{(I-II)C}$ for both cohesive and adhesive failures obtained from static tests of DCB and CLS specimens with FM-400 adhesive, respectively. Also, the corresponding values for FM-300 and EC 3445 adhesives from previous studies[11] are provided for comparison purposes. This shows that the static fracture strength of a bonded joint with the brittle adhesive under the mixed mode I–II condition is about 20 percent less than its counterpart under mode I for

TABLE III
Fracture energies of three adhesives

	Avg. G_{IC} J/m^2		Avg. $G_{(I-II)C}$ J/m^2	
Adhesive	Cohesive failure	Adhesvie failure	Cohesive failure	Adhesvie failure
FM-400	603	306	474	245
FM-300	933	551	991	—
EC 3445	888	—	848	—

cohesive failure. On the other hand, both of these are equal in the case of a bonded joint with the ductile adhesives. Further, the static fracture strengths of these bonded joints in the case of adhesive failure are considerably lower than their counterparts with cohesive failure.

Cyclic debonding behavior

The measured debond growth rate data for FM-400 adhesive were correlated with the corresponding strain-energy-release rates as shown in Figure 8. These obeyed a relationship of the form

$$\frac{da}{dN} = c(G_I \quad \text{or} \quad G_T)^n \tag{1}$$

where c and n are constants dependent on the material and test environment. The solid lines in Figure 8 showing these relations were fitted to the data by using a least-squares regression analysis. The value of c and n thus obtained from the least-squares fit are given in Table IV along with their counterparts for EC 3445 and

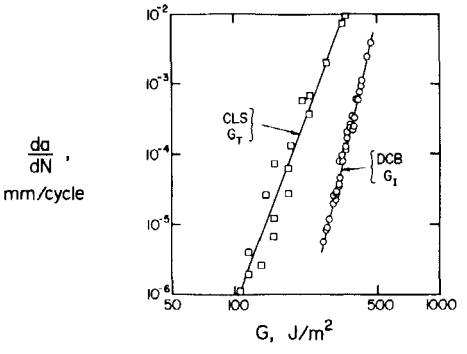

FIGURE 8 Relations between strain-energy-release rates and debond growth rate from two specimens.

TABLE IV
Constants c and n of Eq. (1)

	Mode *I*		Mixed mode *I–II*	
Adhesive	c	n	c	n
FM-400	1.91E-35	12.09	2.24E-22	7.74
FM-300	1.52E-15	4.55	1.52E-15	4.55
EC 3445	1.81E-14	4.34	1.81E-14	4.34

FM-300 adhesives obtained from the previous studies.[10,11] As mentioned earlier, the relationship between strain-energy-release rate and cyclic debond growth rate in ductile adhesives remains unchanged from mixed mode *I–II* to opening-mode *I*. However, this is not the case with the brittle adhesive. This comparison clearly shows that the total strain-energy-release is not the criterion for cyclic debond growth in brittle adhesive as was observed in the ductile adhesive. The primary contribution of mixed mode fatigue loading in the brittle adhesive was the reduction in the debond growth resistance and the exponent, n, as shown in Figure 8 and Table IV. This, thus, leads to the considerable decrease in fatigue threshold value, G_{th} (defined here arbitrarily the strain-energy-release rate corrsponding to $da/dN = 10^{-6}$ mm/cycle) under mixed mode loading when compared with opening mode loading in the case of the brittle adhesive.

The energy absorbed per cycle was more under mixed mode loading than opening mode in the brittle adhesive. Hence, the micro- mechanical damage mechanisms which control debond growth are more degrading when the brittle adhesive is subjected to mixed mode loading. This can be attributed to the type of reinforcement used (rigid particulate, *i.e.*, aluminium filler) in the brittle adhesive to increase its strength. On the other hand, in the ductile adhesives, the reinforcement was a flexible particulate, *i.e.* rubber. This flexible particulate permitted an equal amount of energy absorption per fatigue cycle under both mixed mode *I–II* and mode *I* loadings, which resulted in the same value fo fatigue threshold value and debond growth exponent, n.

Further, the comparison of cyclic debond behavior between softer but more ductile *versus* harder but more brittle adhesives shows that the former will experience more hysteresis per cycle (more energy absorbed), and hence more micro-damage at the crack tip is likely. This phenomenon thus reduces the fatigue resistance of the softer but ductile adhesive in comparison to the harder but brittle adhesive. This feature is shown in Figure 9 where debond growth resistance is replotted in terms of the corresponding static fracture strength, G_{IC} or $G_{(I-II)C}$. This comparison clearly shows that the relative fatigue resistance and threshold value for cyclic debonding in terms of its original static strength is higher in the brittle adhesive than in the ductile adhesive. Thus, increase in ductility of adhesive may not be beneficial in this context, in spite of its effect in

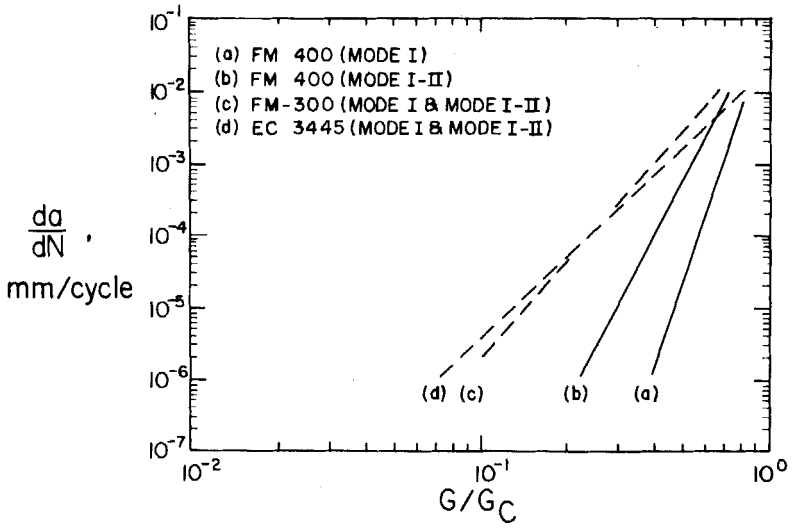

FIGURE 9 Relations between normalized strain-energy-release rate and debond growth rate of different adhesives.

improving the fracture strength, *i.e.* G_{IC} or $G_{(I-II)C}$, under static loading. However, this should be verified for various other brittle and ductile adhesives.

The previous discussion was for the situation when debond growth occurred in the cohesive manner. As mentioned earlier, the debond grew either in a cohesive manner or adhesive manner. Figure 10

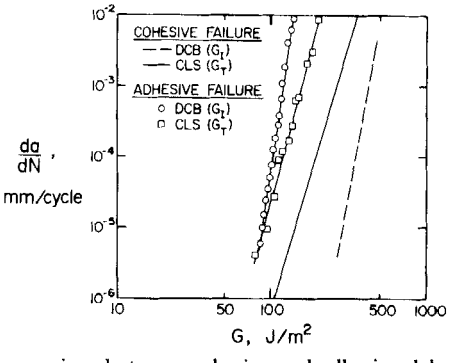

FIGURE 10 Comparison between cohesive and adhesive debond growth rates.

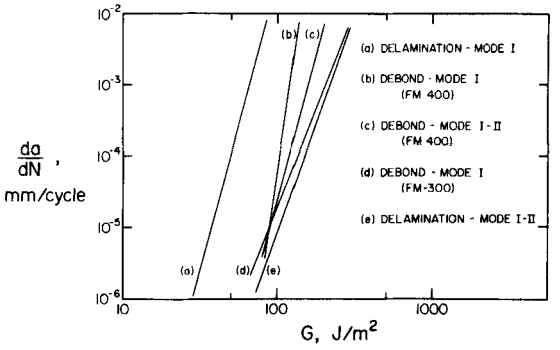

FIGURE 11 Comparison between adhesive debond growth rates and delamination growth rates.

shows the relationships between the measured debond growth rate and strain-energy-release rate from the present DCB and CLS specimens (with FM-400 adhesive) from adhesive failure. Also, the corresponding relationships for cohesive failure are shown in this figure. When these debond growth relations for interfacial failure are compared with their counterparts for cohesive failure, it can be observed that there is a shift in these relations. This shift is towards the left which physically means that there is a several-fold reduction in the fatigue resistance of the bonded joint in case failure occurs in the adhesive manner. Figure 11 shows cyclic delamination growth relationships of the composite adherends used in the tested specimens, *i.e.* graphite/epoxy (T300/5200) for mode *I* and mixed-mode *I-II* from a previous study[16] along with adhesive debond growth relations from the present study. Also, the corresponding relationship for adhesive failure with FM-300 adhesvie from the previous study[11] is shown in this figure. This comparison clearly shows that fatigue strength of interfacial failure in these bonded joints is about of the same order as that of cyclic delamination growth of adherend composite under mixed-mode *I–II* loading especially at low debond growth rates.

CONCLUDING REMARKS

A study of composite-to-composite bonded joints with a brittle adhesive was conducted to characterize the debond growth mechan-

ism under mode *I* and mixed mode *I–II* static and fatigue loadings. The bonded system consisted of graphite/epoxy adherends (T300/5208) bonded with FM-400 adhesive. Two specimen types were tested: (1) a double-cantilever-beam specimen for mode *I* loading and (2) a cracked-lap-shear specimen for mixed mode *I–II* loading. The following conclusions were obtained from this study:

1) The total strain-energy-release rate is not the criterion for cohesive debond growth under static and fatigue loading in the brittle adhesive as observed in the ductile adhesive.

2) There is a considerable reduction in the cyclic debond growth resistance in mixed mode fatigue loading in comparison to opening mode fatigue loading in the case of the brittle adhesive.

3) The relative fatigue resistance and threshold value of cyclic debond growth in terms of its static fracture strength is higher in the brittle adhesive than its counterpart in the ductile adhesive.

Acknowledgement

The work reported was performed at University of Missouri-Rolla under the sponsorship of NASA Langley Research Center, Hampton, Virginia. The authors wish to acknowledge the support and encouragement of Dr. W. S. Johnson, NASA Langley Research Center, during the course of this investigation.

References

1. G. L. Roderick, R. A. Everett, Jr., and J. H. Crews, Jr., in *Fatigue of Composite Materials*, ASTM STP 569 (Am. Socy. for Testing and Materials, Philadelphia, 1975), pp. 295–306.
2. S. Mostovoy and E. J. Ripling, in *Adhesion Science and Technology, 9B* (Plenum Press, N.Y., 1975), pp. 513–562.
3. J. A. Marceau, J. C. McMillan and W. M. Scardino, *Proc. of 22nd Nat. SAMPE Symp. and Exhibition*, **22,** 64–80 (1977).
4. D. A. Jablonski, *J. Adhesion* **12,** 125–143 (1980).
5. T. R. Brussat and S. T. Chiu, *J. Eng. Materials and Technology* **100,** 39–45 (1978).
6. J. Romanko, K. M. Liechti and W. G. Knauss, *AFWAL-TR-82-4139,* Air Force Wright Aeronautical Laboratories, November 1982.
7. C. Lin and K. M. Liechti, *Engineering Mechanics Research Laboratory Report NO. 85/6,* The University of Texas at Austin, August 1985.
8. R. A. Everett, Jr. and W. S. Johnson, in *Delamination and Debonding of Materials,* ASTM STP 876 (Amer. Soc. for Testing and Materials, Philadelphia, 1985), pp. 267–281.
9. R. A. Everett, Jr., *Adhesives Age* **26**(5), 24–29 (1983).
10. S. Mall, W. S. Johnson and R. A. Everett, Jr., in *Adhesive Joints: Their*

Formation, Characteristics, and Testing (Plenum Press, New York, 1984), pp. 639–658.
11. S. Mall and W. S. Johnson, in *Composite Materials: Testing and Design (Seventh Conference)*, ASTM STP 893 (Amer. Soc. for Testing and Materials, Philadelphia, 1986), pp. 322–334.
12. S. Mall, M. A. Rezaizadeh and G. Ramamurthy, *J. Eng. Materials and Technology* **109,** 17–21 (1987).
13. J. D. Whitcomb and B. Dattaguru, *NASA TM 85734,* Jan. 1984.
14. E. F. Rybicki and M. F. Kanninen, *Eng. Fracture Mechanics* **9,** 931–938 (1977).
15. E. C. Francis and D. Gutierrez-Lemini, in *Adhesive Joints: Their Fromation, Characteristics, and Testing* (Plenum Press, New York, 1984), pp. 639–658.
16. R. L. Ramkumar and J. D. Whitcomb, in *Delamination and Debonding of Materials,* ASTM STP 876 (Amer. Soc. for Testing and Materials, Philadelphia, 1985), pp. 315–335.